Molecular Therapy
Original Article

# Therapeutic role of ursodeoxycholic acid in colitis-associated cancer via gut microbiota modulation

Qilang He,[1,2,3] Jinjie Wu,[1,2,3] Jia Ke,[1,2,3] Qiang Zhang,[1,2] Wanyi Zeng,[1,2] Zhanhao Luo,[1,2] Junli Gong,[1,2] Yuan Chen,[1] Zhen He,[1,2] and Ping Lan[1,2]

[1]The Sixth Affiliated Hospital, School of Medicine, Sun Yat-sen University, Guangzhou, 510655 Guangdong, China; [2]Guangdong Provincial Key Laboratory of Colorectal and Pelvic Floor Diseases, Guangdong Institute of Gastroenterology, Guangzhou, 510655 Guangdong, China

**Inflammatory bowel disease (IBD) is a predisposing factor for colitis-associated cancer (CAC). The association between bile acids and the gut microbiota has been demonstrated in colon neoplasia; however, the effect of ursodeoxycholic acid (UDCA) on gut microbiota alteration in development of colitis and CAC is unknown. Our analysis of publicly available datasets demonstrated the association of UDCA treatment and accumulation of *Akkermansia*. UDCA-mediated alleviation of DSS-induced colitis was microbially dependent. UDCA treatment significantly upregulated *Akkermansia* colonization in a mouse model. Colonization of *Akkermansia* was associated with enhancement of the mucus layer upon UDCA treatment as well as activation of bile acid receptors in macrophages. UDCA played a role in CAC prevention and treatment in the AOM-DSS and $Apc^{Min/+}$-DSS models through downregulation of inflammation and accumulation of *Akkermansia*. This study suggests that UDCA intervention could reshape intestinal gut homeostasis, facilitating colonization of *Akkermansia* and preventing and treating colitis and CAC.**

## INTRODUCTION

Colorectal cancer (CRC) is one of the most common malignancies and a leading cause of mortality worldwide.[1] The inflammatory response in the gut is a key driver of CRC development.[2] Colitis-associated cancer (CAC) is a subtype of CRC that emphasizes the role of inflammation in tumorigenesis. Inflammatory bowel disease (IBD), particularly ulcerative colitis (UC) and Crohn's disease, have been suggested as predisposing factors for CAC.[3] A considerable number of patients with IBD still require colectomy for their refractory disease or even intestinal neoplasia.[4,5] Therefore, targeted intervention for colitis is a potential strategy for prophylaxis and treatment of CAC.

Previous studies have revealed the important role of the microbiota in intestinal homeostasis.[6,7] Emerging evidence demonstrates that chronic persistent inflammatory stimulation in response to microbial dysbiosis, such as upregulated colonization of pathogens and downregulated colonization of probiotics, could mediate development of colitis and even CAC.[8,9] Therefore, modulation of the microbiota may be critical for treatment of CAC.

Bile acids (BAs) are important microbial metabolites that modulate homeostasis of the gut immune microenvironment.[10,11] A recent study demonstrated that alteration of symbionts or diet could influence BA pools in the gut and therefore decrease the proportion of $ROR\gamma^{+}$ regulatory T cells (Treg cells) via the vitamin D receptor signaling pathway.[10] Another study revealed that administration of 3-oxo-lithocholic acid and isoallo-lithocholic acid to mice reduced differentiation of T helper 17 cells (Th17 cells) but induced the differentiation of Treg cells in the intestinal lamina propria.[11] It is well known that an aberrant balance of Th17 and Treg cells is associated with progression of IBD, emphasizing the significant role of BAs in inflammatory response. Ursodeoxycholic acid (UDCA), an important BA, has been approved as a standard treatment for primary biliary cholangitis.[12] A previous study showed that UDCA treatment improves dysplasia in patients with IBD and reduces the risk of adenoma recurrence,[13] and application of UDCA has been shown to significantly reduce the risk of advanced adenoma through modulation of the gut microbiome.[13] However, the relationship between UDCA and alteration of the gut microbiota in CAC development remains to be well characterized.

In this study, we postulated that application of UDCA might suppress colitis and CAC via alteration of the gut microbiota, particularly accumulation of *Akkermansia*. To test this hypothesis, different mouse models were used to evaluate the therapeutic potential of UDCA in development of colitis and CAC. We conducted antibiotic and fecal microbiota transplantation (FMT) experiments to examine the effect

Received 22 March 2022; accepted 25 October 2022;
https://doi.org/10.1016/j.ymthe.2022.10.014.

[3]These authors contributed equally

**Correspondence:** Zhen He, Department of Colorectal Surgery, The Sixth Affiliated Hospital of Sun Yat-sen University, Guangzhou, Guangdong 510655, China.
**E-mail:** hezh5@mail.sysu.edu.cn
**Correspondence:** Ping Lan, Department of Colorectal Surgery, The Sixth Affiliated Hospital of Sun Yat-sen University, Guangzhou, Guangdong 510655, China.
**E-mail:** lanping@mail.sysu.edu.cn

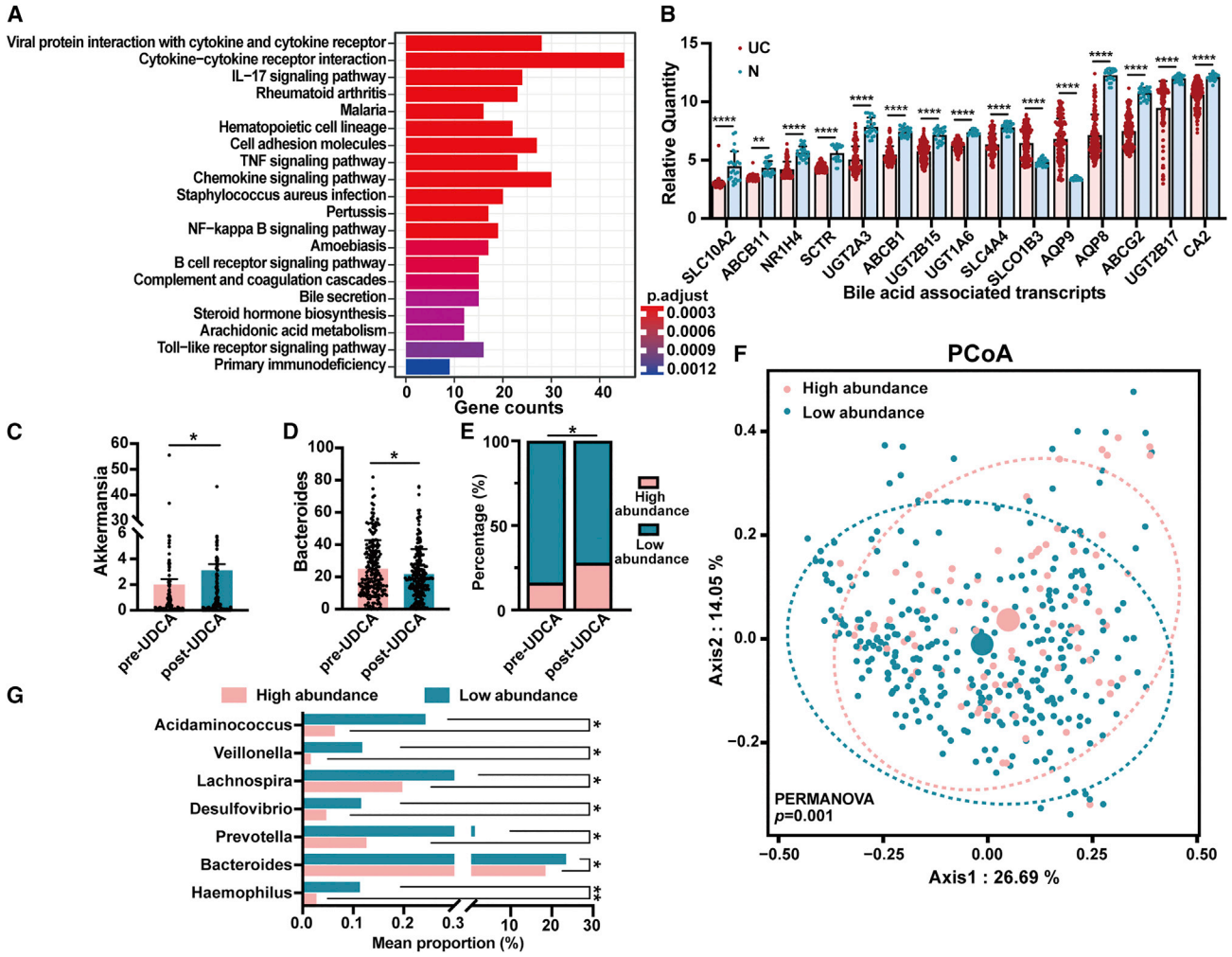


**Figure 1. Ursodeoxycholic acid (UDCA) treatment is associated with accumulation of *Akkermansia***

(A) Pathway analysis of the public transcriptional ulcerative colitis (UC) cohort containing 159 patients with UC and 24 normal control individuals. (B) Significantly altered expression of various BA-associated transcripts in patients with UC compared with that in normal control (N) individuals. (C and D) UDCA treatment significantly upregulated the abundance of *Akkermansia* (C) and downregulated the abundance of *Bacteroides* spp. (D). (E) With an average as cutoff, high abundance of *Akkermansia* was associated with UDCA treatment. (F) Distinct characteristics of the microbiome between patients with high and low abundances of *Akkermansia*. (G) Differential abundance of several genera (adjusted $p < 0.05$) between patients with high and low abundance of *Akkermansia*. *$p < 0.05$, **$p < 0.01$, ***$p < 0.001$, ****$p < 0.0001$. Two-tailed Student's t test (C and D); two-way ANOVA after Tukey's multiple comparison test (B); Fisher's exact test (E).

of the gut microbiota on the therapeutic efficacy of UDCA. The current study demonstrates the role of UDCA in suppression of colitis and CAC, providing a novel strategy for disease prophylaxis and treatment.

## RESULTS

### Clinical application of UDCA was associated with accumulation of *Akkermansia*

To characterize the significance of BAs in colitis, a publicly available transcriptional dataset of a UC cohort, including 159 colon mucosa biopsies with UC and 24 normal controls (GSE87473 and GSE92415), was re-analyzed in our study. Differential analysis of this dataset identified 180 differentially expressed genes (adjusted $p < 0.05$). In addition to inflammation-associated pathways, pathway analysis also revealed that the pathway of bile secretion[14,15] was significantly associated with development of IBD (Figure 1A). Multiple genes associated with BA metabolism were significantly downregulated in patients with UC (Figure 1B), suggesting therapeutic potential of BAs in patients with colitis.

Previous studies have demonstrated that aberrant metabolism of BAs in colitis is associated with dysbiosis.[16] To evaluate the influence of BAs on the microbiome, the fecal microbiome of a clinical cohort of 198 participants undergoing UDCA treatment was analyzed (SRP181937). UDCA treatment significantly enriched the abundance of *Akkermansia* (Figure 1C), whereas *Bacteroides* was significantly

reduced (Figure 1D). With the average of abundance of *Akkermansia* as a cutoff, patients were divided into two groups based on the abundance of *Akkermansia*: a high-abundance group and a low-abundance group. A high proportion of *Akkermansia* was significantly associated with UDCA treatment (Figure 1E). Participants with a higher abundance of *Akkermansia* exhibited distinct microbial characteristics compared with those with a lower abundance of *Akkermansia* (Permutational multivariate analysis of variance, PERMANOVA, $p = 0.001$) (Figure 1F). We next detected differences in the bacterial communities in patients with a higher abundance of *Akkermansia*. Accumulation of *Akkermansia* in the gut was associated with significant downregulation of various commensals, such as *Haemophilus*, *Bacteroides*, *Prevotella*, and *Desulfovibrio* (Figure 1G), which have been described previously to mediate colitis.[17–19] These data indicate that UDCA treatment is associated with accumulation of *Akkermansia*.

### UDCA treatment of colitis is associated with accumulation of probiotics in mice

To evaluate the effect of UDCA on colitis, a dextran sodium sulfate (DSS)-induced colitis mouse model was used in combination with daily gavage of UDCA (Figure 2A). DSS-induced colitis, as measured by weight loss, colon length, and disease activity index (DAI), was significantly ameliorated in mice treated with UDCA compared with control group mice (Figures 2B–2E). Histological assessment of colonic inflammation was characterized by decreased mucosal erosion, crypt destruction, and inflammatory cell infiltration in mice treated with UDCA compared with control group mice (Figures 2F and 2G). Consistent with the histological improvement, the mRNA expression of pro-inflammatory cytokines interleukin-1β (IL-1β), IL-6, and tumor necrosis factor alpha (TNF-α) in terminal ileum was significantly decreased in mice treated with UDCA (Figure 2H). These data indicate therapeutic efficacy of UDCA in colitis development.

To validate the UDCA-induced alteration of the microbiome, the characteristics of the microbiome from mice treated with UDCA were determined using 16S ribosomal RNA gene sequencing. Similar to most of the current data,[20] the diversity of the gut microbiome significantly decreased after UDCA treatment (Figure 2I). Taxonomic analysis of the microbiome using principal coordinate analysis (PCoA) showed significant clustering and separation between the microbiome of the UDCA-treated and control groups (PERMANOVA, $p = 0.001$) (Figure 2J). Generally, the phyla Bacteroidetes and Proteobacteria were downregulated, whereas the phylum Verrucomicrobia was upregulated with use of UDCA (Figure 2K). We subsequently applied linear discriminant analysis of effect size (LEfSe) to detect marked differences in the predominance of bacterial communities in UDCA-treated mice. Multiple genera of potential probiotics, including *Akkermansia* and *Lactobacillus*, were significantly enriched in UDCA-treated mice (Figure 2L). We also validated the abundance of these probiotics by qPCR. As expected, the relative abundance of *Akkermansia* was significantly high in the feces of the UDCA-treated group (Figure 2M). Phylogenetic investigation of communities by reconstruction of unobserved states (PICRUSt) also indicated involvement of the primary BA biosynthesis and peroxisome proliferator-activated receptor signaling pathways (Figures S1A and S1B), which are common relevant pathways, upon application of BAs, as described previously.[21] These data demonstrate that the therapeutic effect of UDCA on colitis is associated with an alteration in the gut microbiome.

### The therapeutic potential of UDCA is microbially dependent

To explore the role of the gut microbiota in UDCA treatment, we established a mouse model with antibiotic intervention. Mice were administered an antibiotic cocktail containing ampicillin, vancomycin, neomycin, and metronidazole in their drinking water throughout the experiment. After 4 days of antibiotic exposure, mice were challenged with DSS in combination with daily gavage of UDCA (Figure 3A). Exacerbation of weight loss, shortening of colon length, and changes in DAI in UDCA-treated mice were significantly worse after antibiotic intervention (Figures 3B–3E). Histopathological parameters were also characterized by increased mucosal erosion, crypt destruction, and inflammatory cell infiltration in UDCA-treated mice with antibiotic intervention (Figures 3F and 3G). Similarly, various inflammatory cytokines, such as IL-1β, IL-6, and TNF-α, were upregulated in intestinal tissues from UDCA-treated mice with antibiotic intervention (Figures S2A–S2C). The quantity of *Akkermansia* was significantly higher in feces from the UDCA-treated group but not detected in feces from the antibiotic-treated group (Figure S2D). These data indicate that the therapeutic effect of UDCA on colitis was impaired by depletion of the gut microbiota.

To confirm whether alteration of the gut microbial structure driven by UDCA may have a causal effect on colitis development, we performed FMT experiments. The microbiota was collected from donor mice treated with UDCA or normal saline (microbial donor [MD]) and subsequently transferred to specific pathogen-free (SPF) recipient mice (microbial recipient [MR]) challenged with 3% DSS (Figure 3H). Fecal microbiota from UDCA-treated MD mice significantly ameliorated colitis in MR mice, whereas MR mice gavaged with a placebo fecal microbiota exhibited worse weight loss, shortened colon length, and a higher DAI score (Figures 3I–3L). Histological parameters also improved in mice that received a fecal microbiota from UDCA-treated donors (Figures 3M and 3N). The intestinal mRNA expression of IL-1β and TNF-α was significantly downregulated in MR mice that received a fecal microbiota from UDCA-treated donors compared with that in mice that received a placebo microbiota (Figures S2E and S2F). The colonic protein expression of various tight junction molecules (such as ZO-1, claudin 3, and occludin) in MR mice was also restored after receiving a FMT from UDCA-treated MD mice (Figure S2G). 16S rRNA gene sequencing revealed a distinct microbiotic pattern in mice with FMT intervention, and significant enrichment of *Akkermansia* was found in recipient mice with feces from UDCA-treated MD mice (Figures S2H and S2I). Validation by qPCR also demonstrated that a significant accumulation of *Akkermansia* was present in donor and recipient mice (Figures 3O and 3P),

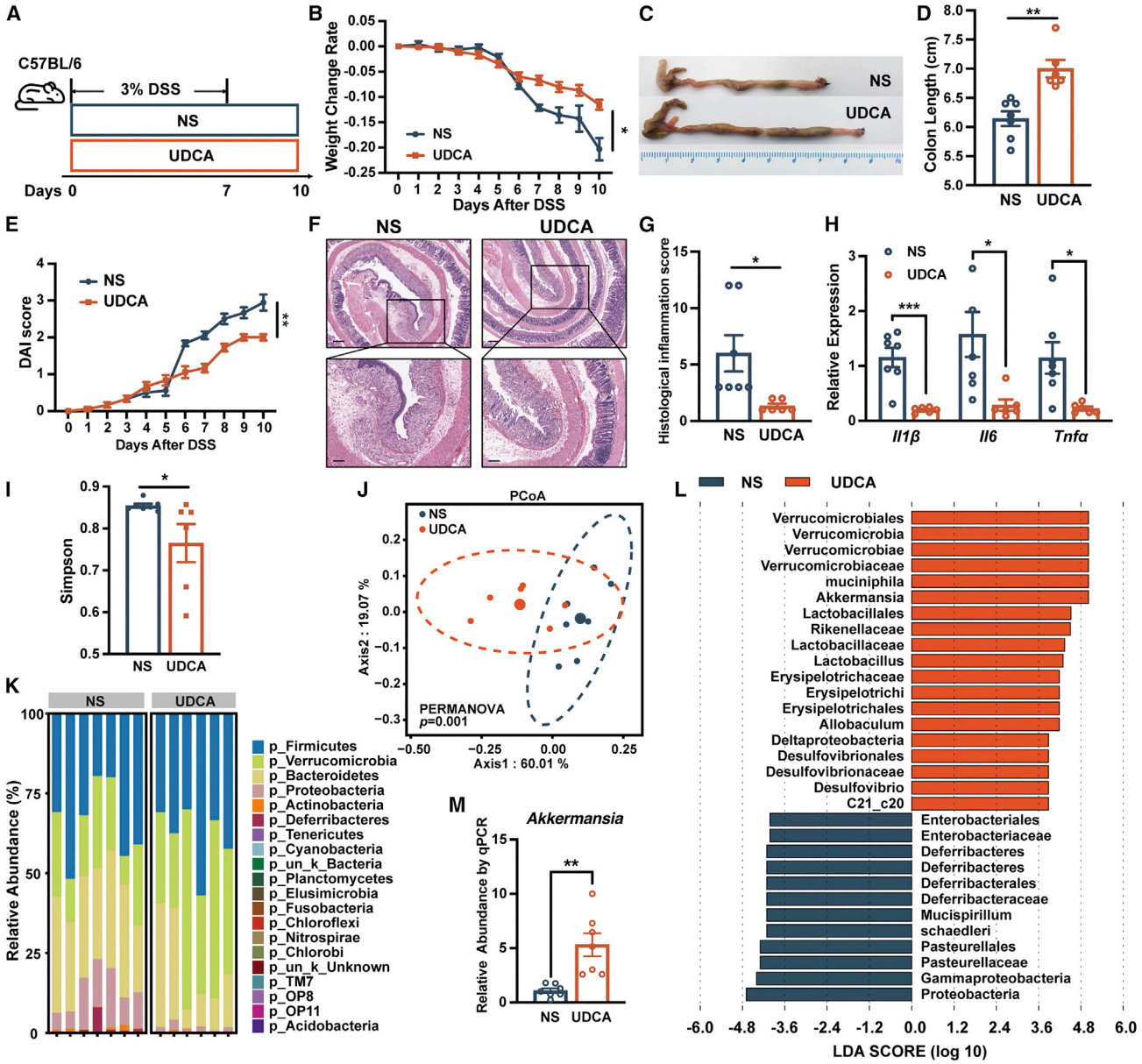


**Figure 2. UDCA-mediated suppression of colitis was associated with gut microbiome alteration**

(A) C57BL/6 mice were exposed to 3% dextran sodium sulfate (DSS) for 7 days, followed by regular water for 3 days. The mice were gavaged daily with UDCA (n = 6) or normal saline (NS) (n = 7) until being euthanized. (B) Changes in body weight after 3% DSS administration. (C–G) Representative colon (C), colon length (D), disease activity index (DAI) (E), representative colonic histological images (scale bars, 250 μm [top] and 100 μm [bottom]) (F), and colonic histological score (G) in mice treated with UDCA or NS. (H) Quantitative PCR detected intestinal RNA levels of pro-inflammatory cytokines (IL-1β, IL-6, and TNF-α) in mice treated with UDCA or NS. (I) Alpha diversity of the gut microbiome in mice treated with UDCA or NS. (J) Principal coordinates analysis (PCoA) revealed separation of the gut microbiome in mice treated with UDCA or NS (Adonis p = 0.001). (K) General landscape of the microbiome at the phylum level in mice treated with UDCA or NS. (L) Differentially abundant bacterial communities between UDCA-treated and NS-treated mice using linear discriminant analysis of effect size (LEfSe) (LDA > 4). (M) The quantity of *Akkermansia* in feces from mice treated with UDCA or NS was assessed by qPCR. *p < 0.05, **p < 0.01, ***p < 0.001, ****p < 0.0001. Two-tailed Student's t test (D, G, H, I, and M); two-way ANOVA after Tukey's multiple comparison test (D and E).

indicating alleviation of colitis by UDCA-mediated accumulation of *Akkermansia*. These data demonstrate that the therapeutic potential of UDCA in colitis depends on the gut microbiota, especially increased colonization of *Akkermansia*.

### UDCA induces accumulation of *Akkermansia* to alleviate colitis via enhancement of the mucous layer

A previous study demonstrated the predilection of *Akkermansia* in the mucus layer.[22] We found that a high abundance of *Akkermansia*

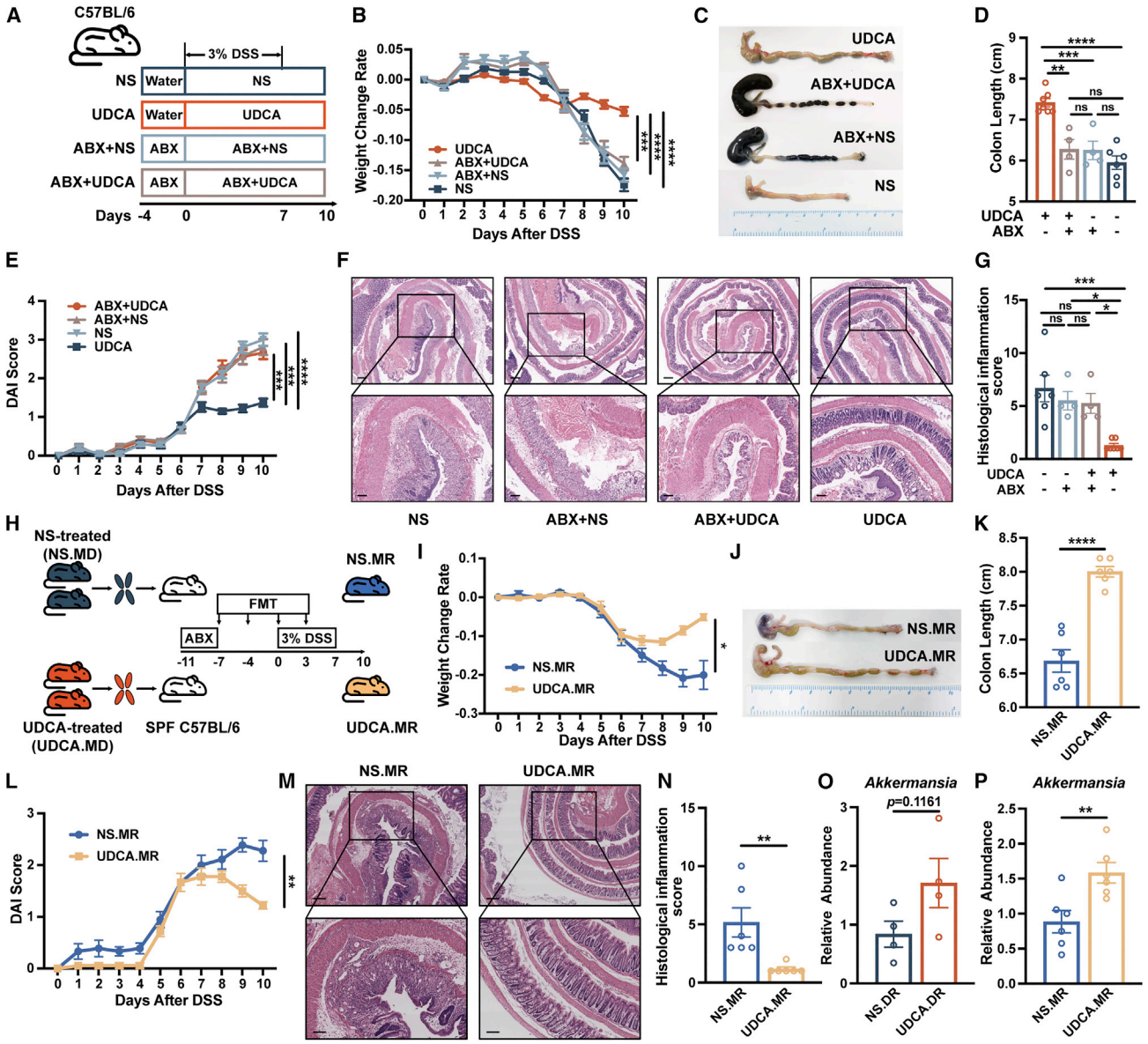


**Figure 3. The therapeutic potential of UDCA is dependent on the existence of the gut microbiota**

(A) C57BL/6 mice were treated with water for 4 days and subsequently exposed to 3% DSS for 7 days, followed by regular water for 3 days. These mice were gavaged daily with UDCA (UDCA, n = 7; antibiotic cocktail [ABX] + UDCA, n = 4) or NS (NS, n = 6; ABX + NS, n = 4) until being euthanized. To deplete the gut microbiota, mice were treated with ABX until being euthanized. (B) Changes in body weight after 3% DSS administration. (C–G) Representative colon (C), colon length (D), DAI (E), representative colonic histological images (scale bars, 250 μm [top] and 100 μm [bottom]) (F), and colonic histological score (G) in mice treated with UDCA or NS. (H) Schematic of fecal microbiota transplantation (FMT). Fresh feces from NS-treated or UDCA-treated donors (NS.MD or UDCA.MD) (NS.MD, n = 4; UDCA.MD, n = 4) were used as a source for NS-treated or UDCA-treated recipient mice (NS.MR or UDCA.MR) (NS.MR, n = 6; UDCA.MR, n = 6), respectively. After 3 days of ABX treatment and a 24-h washout period, the recipient mice were orally treated with a washed donor fecal microbiota twice a week. After 1 week of FMT, mice were exposed to 3% DSS for 7 days, followed by regular water for 3 days. (I) Changes in body weight after 3% DSS administration. (J–N) Representative colon (J), colon length (K), DAI (L), representative colonic histological images (scale bars, 250 μm [top] and 100 μm [bottom]) (M), and colonic histological score (N) in recipient mice treated with feces from donor mice. (O and P) Relative abundance of *Akkermansia* in feces from donor (O) and recipient mice (P). *$p < 0.05$, **$p < 0.01$, ***$p < 0.001$, ****$p < 0.0001$. One-way ANOVA after Tukey's multiple comparisons test (D and G); two-way ANOVA after Tukey's multiple comparisons test (B, E, I, and L); two-tailed Student's t test (K and N–P).

was significantly positively correlated with the mRNA level of *Muc2* in mouse intestinal tissue (Figure S3A), implying a role of the mucus layer in UDCA-induced accumulation of *Akkermansia*. To confirm how UDCA mediates accumulation of *Akkermansia*, we assessed changes in the intestinal barrier after UDCA treatment. The expression of several intestinal barrier molecules (*Muc2*, *occludin*, and

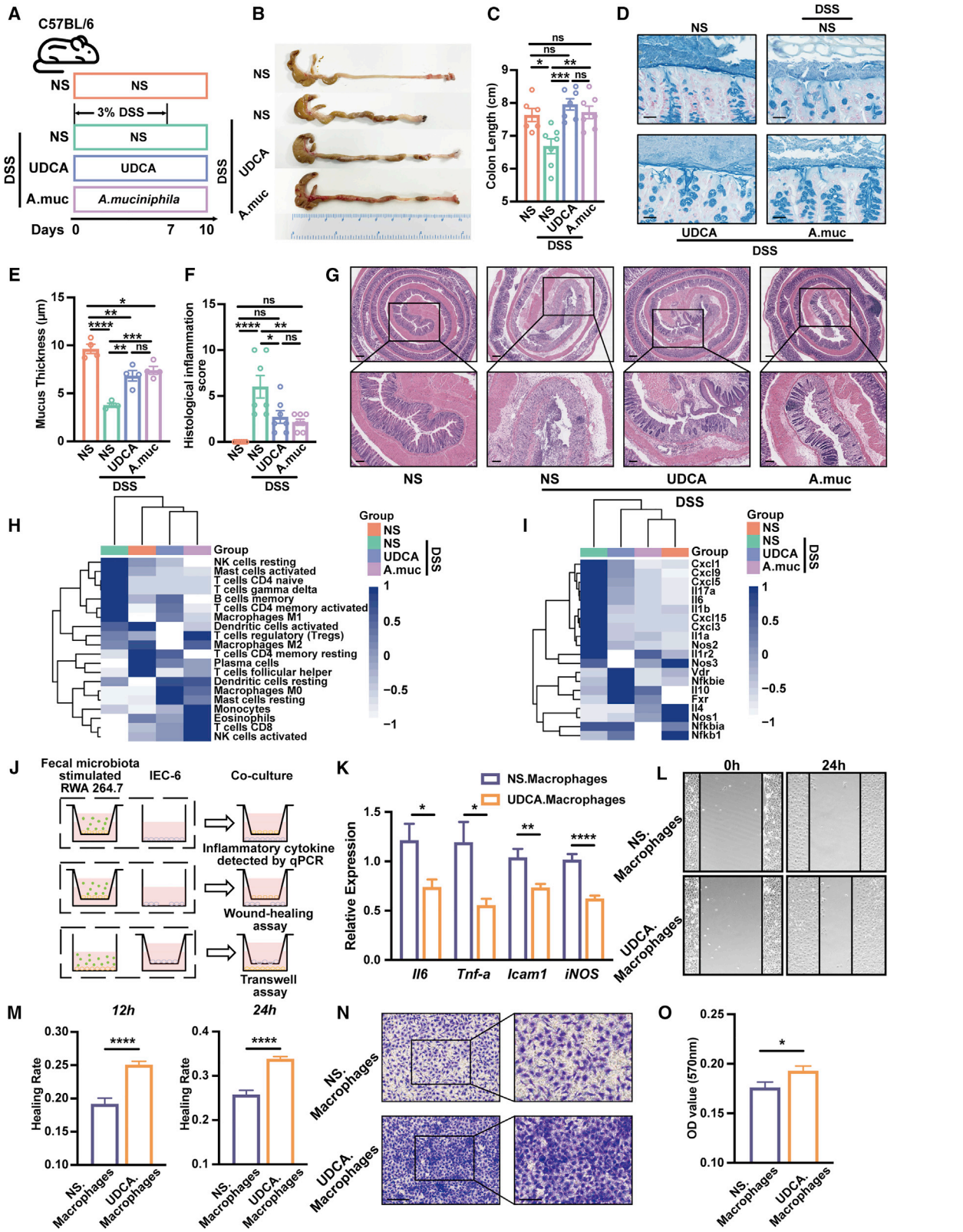


*(legend on next page)*

*ZO-1*) in the intestinal tissue was significantly upregulated in mice treated with UDCA (Figure S3B). Specifically, multiple mucus-associated transcripts, including *Muc2*, *Muc3*, *Muc4*, *Muc13*, *Tff3*, and *Fc-γ-Bp*, were significantly upregulated in the colonic tissue of mice treated with UDCA (Figure S3C). Alcian blue staining revealed a significantly higher thickness of the mucus layer in UDCA-treated mice than in the control groups (Figures S3D and S3E).

To investigate the role of *Akkermansia muciniphila* enriched by UDCA in intestinal inflammation, we colonized *A. muciniphila* in mice with DSS intervention (Figure 4A). The colon length in mice treated with *A. muciniphila* was similar to that in mice with UDCA administration, which were both significantly improved compared with the control group (Figures 4B and 4C). Compared with mice with DSS intervention, a significantly increased thickness of the mucous layer and improved characteristics of histological parameters were also found in mice treated with *A. muciniphila* or UDCA (Figures 4D–4G). These data suggest that UDCA treatment created an environment characterized by enhancement of the mucus layer, facilitating accumulation of *Akkermansia* to alleviate colitis in mice.

### UDCA-induced *Akkermansia* in colitis is associated with activation of BA receptors in macrophages

To assess the underlying mechanism of *Akkermansia* accumulation in colitis, multiple BA receptors in the terminal ileum from mice with antibiotics or FMT treatment described above (Figures 3A and 3H) were detected using qPCR. Highly significant upregulation of BA receptors, such as farnesoid X receptor (*Fxr*) and pregnane X receptor (*Pxr*), was observed in the intestine of UDCA-treated mice, whereas these receptors were significantly downregulated after treatment with the antibiotic cocktail (Figures S4A and S4B). Similar results from the FMT experiments emphasized microbiota-dependent upregulation of *Fxr* and *Pxr* after UDCA treatment (Figures S4C and S4D). Mice treated with UDCA or a UDCA-induced microbiota were also associated with upregulation of small heterodimer partner (*Shp*), a downstream target gene of *Fxr* (Figures S4E and S4F). However, the mRNA expression levels of takeda G protein-coupled receptor 5 (*Tgr5*) and vitamin D receptor (*Vdr*) upon UDCA administration were comparable between mice treated with antibiotics and untreated mice (Figures S4G–S4J). We found that upregulation of *Fxr* in mice that received a fecal microbiota from UDCA-treated donors was associated with downregulation of *Icam1* and *iNos* (Figures S4K and S4L), indicating suppression of nuclear factor κB (NF-κB) signaling pathways after UDCA treatment.

A previous study demonstrated involvement of the FXR-NF-κB pathway in macrophages.[23] Hence, we performed RNA sequencing, using colonic tissue from mice treated with UDCA or *Akkermansia* (Figures 4H and 4I). To depict the immune contexture, we evaluated the relative abundance of different immune cells from gene expression profiles using the cell-type identification by estimating relative subsets of RNA transcripts (CIBERSORT). The pattern of immune composition was similar in mice with UDCA treatment or *Akkermansia* intervention (Figure 4H). As an important antigen-presenting cells, macrophage signals associated with the M1 phenotype were downregulated in mice with UDCA treatment or *Akkermansia* intervention. Specifically, increased M2 phenotype signals of macrophages were observed in mice from the *Akkermansia* group. Similarly, various inflammatory cytokines were downregulated in mice gavaged with UDCA or *Akkermansia* (Figure 4I). The BA receptors (*Fxr* and *Vdr*) were also found to be upregulated, whereas expression of several transcripts associated with the NF-κB pathway was obviously decreased in mice with *Akkermansia* treatment. We verified this mechanism in the macrophage cell line RAW264.7. Compared with macrophages stimulated by feces from normal saline (NS)-treated mice, macrophages stimulated by a fecal microbiota from mice treated with UDCA demonstrated upregulation of *Fxr*, *Pxr*, and *Shp* and downregulation of intercellular ddhesion molecule 1 (*Icam1*) (Figures S4M–S4P). These data suggest a potential mechanism by which microbiota-mediated activation of BA receptors is associated with suppression of the NF-κB signaling pathway in macrophages.

### UDCA treatment improves CAC by modulation of the microbiota

Chronic colonic inflammation is an important risk factor for carcinogenesis. We subsequently developed an *in vitro* co-culture system of macrophages (RAW264.7) and intestinal epithelial cells (IEC-6) to explore the role of UDCA-associated microbiotas in epithelial inflammation (Figure 4J). We found that macrophages stimulated by feces from UDCA-treated mice (UDCA.macrophages) significantly reduced expression of inflammatory cytokines (IL-6, TNF-α) and NF-κB target genes (*Icam1* and *iNOS*) in IEC-6 cells (Figure 4K).

**Figure 4. UDCA-induced *Akkermansia* in colitis is associated with activation of BA receptors in macrophages**

(A) C57BL/6 mice were exposed to 3% DSS for 7 days, followed by regular water for 3 days. These mice were gavaged daily with UDCA (n = 7), *A. muciniphila* (n = 7), or NS (n = 7) until being euthanized. As controls, mice were gavaged with NS without DSS treatment (n = 6). (B–G) Representative colon (B), colon length (C), representative mucus layer by Alcian blue staining (scale bar, 25 μm) (D), and mucus thickness (E), colonic histological score (F), representative colonic histological images (scale bars, 250 μm [top] and 100 μm [bottom]) (G) in mice treated with NS, UDCA, or *A. muciniphila*. (H) The distribution of intestinal immune cells was analyzed on the basis of the transcriptome. (I) Relative abundance of several transcripts associated with inflammatory cytokines, BA receptors, and the NF-κB signaling pathway. (J) Schematic of the co-culture experiment of IEC-6 and RAW 264.7 cells stimulated by fecal microbiotas from UDCA- or NS-treated mice (UDCA.macrophages or NS.macrophages). (K) Relative expression of inflammatory cytokines in IEC-6 cells after co-culture for 24 h with stimulated RAW 264.7 cells. (L) Representative images acquired 0 and 24 h after wounding of IEC-6 cells co-cultured with UDCA.macrophages or NS.macrophages. The lines define the areas lacking cells. (M) The percentage of healing area was determined by calculating the healing area at 12 or 24 h with that at time 0 h. (N and O) Representative photographs of the Transwell migration assay of IEC-6 cells co-cultured with UDCA.macrophages or NS.macrophages (N) (scale bars, 200 μm [left] and 100 μm [right]), and the optical density 750 ($OD_{750}$) of crystal violet-stained transmembrane cells dissolved in acetic acid (O). *p < 0.05, **p < 0.01, ***p < 0.001, ****p < 0.0001. One-way ANOVA after Tukey's multiple comparisons test (C, E, and F); two-tailed Student's t test (K, M, and O).

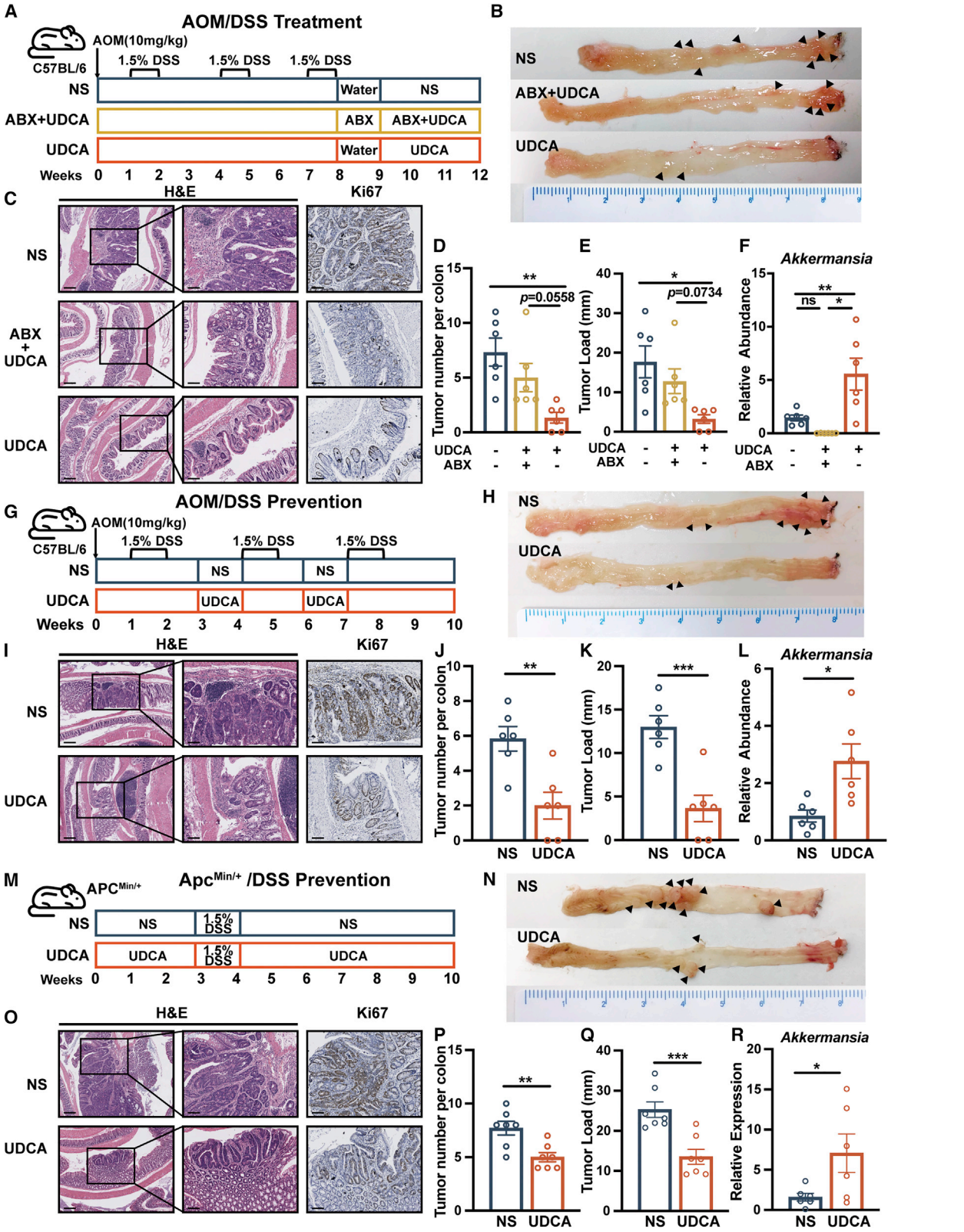


*(legend on next page)*

Healing (Figures 4L and 4M) and migration (Figures 4N and 4O) of IEC-6 cells were promoted by UDCA.macrophages. These data indicated a role of UDCA-associated macrophages in epithelial inflammation, leading to alleviation of CAC.

To evaluate the therapeutic potential of UDCA in CAC, mice were injected with azoxymethane (AOM), a carcinogenic agent, to mimic development of CAC, followed by three cycles of DSS. After challenge with DSS, the mice were treated with UDCA for 3 weeks, as shown in Figure 5A. Macroscopic evaluation of the colon revealed significantly fewer tumors and smaller tumor sizes in mice treated with UDCA (Figures 5B–5E). Several inflammatory cytokines, such as IL-1β, IL-6, and TNF-α, were significantly decreased after UDCA treatment (Figures S5A–S5C). Similar to the immune pattern observed in colitis, UDCA treatment significantly downregulated the mRNA expression of CD80 and CD86 but upregulated CD163 in intestinal tissue (Figures S5D–S5F), indicating that the role of UDCA in CAC development may be associated with modulation of macrophage infiltration. However, this therapeutic effect of UDCA in the CAC model was alleviated after intervention with the antibiotic cocktail (Figures 5B–5E).

In addition to the role of UDCA in CAC treatment, we investigated whether UDCA has a preventive effect on CAC. Mice treated with AOM/DSS were subjected to gavage with UDCA, imitating a pre-clinical model of tumor prevention (Figure 5G). The tumor load in the mice was significantly reduced after UDCA treatment (Figures 5H–5K). As expected, the reduced tumor load was accompanied by downregulation of several inflammatory cytokines in the gut of mice treated with UDCA (Figures S5G–S5I). *Apc*$^{Min/+}$ mice exposed to 1.5% DSS for 1 week, as described previously,[24] were also used to assess the preventive potential of UDCA on CAC. The mice were gavaged with UDCA throughout the experiment (Figure 5M). Consistent with the results in the AOM/DSS model, UDCA reduced the size and number of colonic tumors as well as the levels of various pro-inflammatory cytokines (Figures 5N–5Q and S5J–S5L). The relative abundance of *Akkermansia* in feces was significantly high in mice treated with UDCA (Figures 5F, 5L, and 5R), demonstrating that the therapeutic potential of UDCA in CAC may be mediated by accumulation of *Akkermansia*. These data demonstrated a role of UDCA in prophylaxis and treatment of CAC.

## DISCUSSION

This study highlights that the therapeutic potential of UDCA in colitis and CAC is mediated by accumulation of *Akkermansia* through enhancement of the mucus layer. Our present data demonstrate that application of UDCA-induced alleviation of colitis is microbially dependent. Specifically, accumulation of *Akkermansia* upon UDCA treatment was associated with an increased thickness of the mucus layer. UDCA-induced colonization of *Akkermansia* was accompanied with a downregulated M1 phenotype signal of macrophages and an increased M2 signal in colon tissue. In addition to the therapeutic effect on colitis, we also provide evidence to emphasize the significance of UDCA during prophylaxis and treatment of CAC via modulation of the gut microbiota. We show the potential mechanism by which the altered microbiota, upon UDCA treatment, was associated with activation of the BA receptor and downstream NF-κB signaling pathway in macrophages.

Several studies have demonstrated the essential role of BAs in immune modulation and gut homeostasis.[16] BA-induced immunoregulation has been shown to mediate the prognosis of colitis.[10,11] As a synthetic BA, UDCA is a standard therapeutic strategy for primary biliary cholangitis,[12] indicating its role in suppression of the inflammatory response. Recent studies found that application of UDCA could reduce the risk of CRC in patients with UC, primary sclerosing cholangitis, or primary biliary cirrhosis.[25,26] A large phase III placebo-controlled, randomized trial of UDCA also found a reduced risk of adenoma recurrence with high-grade dysplasia.[27] Some evidence has shown therapeutic significance of UDCA in colitis and colonic neoplasms.[28–31] Similarly, the present study demonstrated that UDCA reduced tumorigenesis in a mouse model, probably through suppression of intestinal inflammation. This evidence emphasizes the clinical significance of UDCA in colitis and CAC.

Previous studies have shown a direct effect of UDCA on colon cancer cells through activation of the TGR5-Yes-associated protein (YAP) axis or oxidative stress.[30,32] In addition to the direct effect, previous studies have shown that the different efficacy of UDCA on advanced adenoma may be related to alteration of the intestinal microbiota.[13,33] BAs are known to have a strong effect on alteration of the gut microbiota. Specifically, cholic acid increased members of *Clostridia* and of

**Figure 5. UDCA application limits CAC by modulation of the microbiota**

(A) Schematic of treatments in azoxymethane (AOM)/DSS-treated mice. After the initial AOM injection (10 mg/kg), three cycles of 1.5% DSS were administered to mice in drinking water. Then mice were gavaged daily with UDCA or NS until being euthanized. To deplete the gut microbiota, mice were treated with ABX until being euthanized. (B) Representative images of macroscopic polyps in the AOM-DSS model throughout disease progression. (C) Representative colonic histological images and representative images of Ki67 immunohistochemical staining in colon tissues; scale bars, 250 μm (left) and 100 μm (center and right). (D and E) Tumor nodules and tumor size in mice treated with UDCA or NS. (F) Relative abundance of *Akkermansia* in feces from mice treated with UDCA or NS. (G) Schematic of treatments in AOM-DSS-treated mice. Mice were gavaged with UDCA after every cycle of DSS administration. (H) Representative images of macroscopic polyps in the AOM-DSS model throughout disease progression. (I) Representative colonic histological images and representative images of Ki67 immunohistochemical staining in colon tissues; scale bars, 250 μm (left) and 100 μm (center and right). (J and K) Tumor nodules and tumor size in mice treated with UDCA or NS. (L) Relative abundance of *Akkermansia* in feces from mice treated with UDCA or NS. (M) Schematic of treatments in *Apc*$^{Min/+}$ mice. After gavage with UDCA or NS for 2 weeks, *Apc*$^{Min/+}$ mice were exposed to 1.5% DSS for 1 week. Mice were gavaged with UDCA or NS for a subsequent 7 weeks. (N) Representative images of macroscopic polyps in the AOM-DSS model throughout disease progression. (O) Representative colonic histological images and representative images of Ki67 immunohistochemical staining in colon tissues; scale bars, 250 μm (left) and 100 μm (center and right). (P and Q) Tumor nodules and tumor size in mice treated with UDCA or NS. (R) Relative abundance of *Akkermansia* in feces from mice treated with UDCA or NS. *$p < 0.05$, **$p < 0.01$, ***$p < 0.001$, ****$p < 0.0001$. One-way ANOVA after Tukey's multiple comparison test (D–F); two-tailed Student's t test (J–L and P–R).

the subclass Erysipelotrichia in rats, with a corresponding loss of members of the phyla Bacteroidetes and Actinobacteria.[34] Deoxycholic acid could directly downregulate colonization of *Bifidobacterium breve* and *Lactobacillus salivarius*.[35] Secondary BAs also promote colonization resistance to *Clostridioides difficile* infection, as demonstrated by the inhibitory effect of *Clostridium sporogenes* on *C. difficile*, with deoxycholic acid acting as the key mediator.[36] Our present data also found that the therapeutic potential of UDCA was microbially dependent, indicating a indirect mechanism of UDCA on colitis and CAC. Although various studies have proposed UDCA-induced modulation of the microbiota,[37] limited evidence has been provided to elucidate the causality of UDCA in changes in the gut microbiota. The present study demonstrated that UDCA drove the accumulation of gut probiotics, especially upregulation of *Akkermansia* and *Lactobacillus*. These two strains are well-known probiotics that have diverse effects on gastrointestinal and metabolic disease.[38–41] However, only *Akkermansia* was found to be significantly upregulated in donor and recipient mice. Our results also suggested that the effect of UDCA on treatment of colitis and CAC relies on accumulation of *Akkermansia*, emphasizing the significance of the microbiome in UDCA indirect efficacy. Elucidation of the *Akkermansia* effect on UDCA-induced regression of colitis and CAC was a novel therapeutic strategy.

However, the underlying mechanism between UDCA and *Akkermansia* accumulation remains unclear. *A. muciniphila* is associated with a low-grade inflammatory tone to protect from specific metabolic disorders and cardiometabolic risk factors.[22] A previous study demonstrated that *A. muciniphila* activates TLR2 through purified membrane proteins to mediate intestinal homeostasis, alleviating the gut inflammatory response.[42] A recent study found that this purified membrane protein from *A. muciniphila* blunted colitis-associated tumorigenesis.[9] Although various studies have concentrated on the interaction between *A. muciniphila* and the host, the precise modulation of *A. muciniphila* in the gut lumen remains a challenge. A previous study confirmed that UDCA could maintain intestinal barrier function and limit mucosal inflammation.[43] Our present study suggests that UDCA application could enhance the intestinal mucus layer and attenuate intestinal inflammation. These changes in the gut microenvironment in response to UDCA treatment are suitable for *A. muciniphila* enrichment. Similarly, a previous study demonstrated a close correlation between *A. muciniphila* and the thickness of the mucus layer,[42] probably through release of microbe-associated molecular patterns and production of short-chain fatty acids.[44–46] Other evidence revealed increased infiltration of M1 macrophages[47] and downregulation of M2 macrophages[8] during CAC development, and elevated colonization of *A. muciniphila* is associated with decreased CD16/32$^{+}$ macrophages in the spleen and mesenteric lymph nodes of colitis mice.[9] Our results also found a downregulated M1 phenotype signal of macrophages in mice treated with UDCA and *A. muciniphila*. An association between increased *A. muciniphila* and inhibition of the NF-κB signaling pathway in macrophages may contribute to activation of BA-associated receptors. Despite the previously described role of BAs in the BA receptor, alteration of the gut microbiota also has a novel effect on activation of several BA receptors during development of colitis.[48,49] However, the causal relationship between *A. muciniphila* and macrophages upon UDCA treatment requires further evaluation. Experiments with gnotobiotic mice are encouraged to validate the role of UDCA and *Akkermansia* in regression of colitis and CAC.

The current study revealed a critical role of UDCA in colitis and CAC that was mediated by alterations in the microbiome. UDCA intervention can reshape intestinal gut homeostasis, facilitating colonization of *Akkermansia* and preventing and even treating colitis and CAC. Elucidation of the relationship between UDCA and the gut microbiome could provide a novel strategy for prophylaxis and treatment of inflammation-associated tumorigenesis.

## MATERIALS AND METHODS

### Clinical cohorts

To evaluate the relationship between colitis and BAs, transcriptome datasets (GSE87473 and GSE92415) of a UC cohort were used in our study. The fecal microbiome from the clinical dataset SRP181937 was used to explore the role of UDCA treatment in microbiome alterations.

### Mice

Six- to eight-week-old male C57BL/6 mice and *APC* $^{Min/+}$ mice were housed under a 12:12 h light:dark cycle in a SPF facility at the Sixth Affiliated Hospital of Sun Yat-Sen University. SPF mice were fed a sterilized laboratory rodent diet (5L0D, LabDiet). Animals were handled in accordance with protocols approved by the Institutional Animal Care and Use Committee (IACUC) at Sun Yat-Sen University.

### Isolation and identification of *A. muciniphila*

For isolation of *A. muciniphila*, fresh mouse feces were homogenized as described previously. Fecal pellets (200–250 mg) were collected in sterile tubes prior to suspension and homogenization in 2 mL of phosphate-buffered saline (PBS) under anaerobic conditions. After serial dilutions, the supernatant was spread onto brain heart infusion (BHI)-supplemented mucin (4 g/L, M378, Sigma, CA) agar plate and incubated overnight under anaerobic conditions for 72 h (80% $N_2$, 10% $H_2$, 10% $CO_2$). Bacterial DNA was extracted from each single colony, and the identity of individual isolates was verified by Sanger sequencing of the V1–V9 regions of the 16S rRNA gene. The following primer set was used for amplifications: 27F 5′-AGAGTTTGATCCTGGCTCAG-3′and 1492R 5′-GGTTACCT TGTTACGACTT-3′. 16S rRNA sequencing was performed using the Illumina MiSeq platform.

### DSS-induced colitis

To induce colitis, C57BL/6 mice were treated with 3% DSS for 7 days, followed by regular water for 3 days. Mice received UDCA or NS treatments daily during the whole experiment. For the antibiotic experiment, SPF mice were treated with a broad-spectrum antibiotic cocktail (ampicillin [0.2 g/L], metronidazole [0.2 g/L], neomycin 0.2

[g/L], and vancomycin [0.1 g/L]) in the drinking water throughout the experiment. After 4-day treatment with antibiotics, mice gavaged with UDCA or NS were challenged with DSS. UDCA was administered daily by oral gavage (50 mg/kg body weight) as described previously.[37] For the *A. muciniphila* colonization experiment, mice were gavaged with *A. muciniphila* (1 × 109 colony-forming units [CFUs]/dose) daily. The animals were monitored for weight loss (0, none; 1, 1%–5%; 2, 5%–10%; 3, 10%–20%; 4, >20%), stool consistency (0, normal stool; 2, loose stool; 4, diarrhea), and hemoccult (0, normal; 2, hemoccult positive; 4, gross blood) during the course of experiments, and averages of these parameters were used to compute the DAI.[50] Mice were sacrificed, and their colon tissues were fixed in 4% paraformaldehyde for H&E staining or modified Carnoy's fixative for Alcian blue staining. DAI and histological analysis were performed as in previous studies.[50,51]

### FMT

SPF C57BL/6 donor mice were treated with UDCA (50 mg/kg body weight) or NS for 2 weeks. The fecal microbiota was prepared under anaerobic conditions as described previously.[52] Fecal pellets (200–250 mg) were collected in sterile tubes prior to suspension and homogenization in 2 mL of PBS previously placed in an anaerobic chamber overnight. After centrifugation at 500 rpm at 4°C for 30 s, bacterially enriched supernatants were collected and centrifuged for 5 min at 4,500 rpm, and the supernatant was discarded; this procedure was repeated three times. The final bacterial pellets were resuspended in 2 mL PBS for gavage (200 μL/mouse). SPF recipient mice were treated with an antibiotic cocktail for 4 days and then gavages with the donor fecal microbiota twice a week before 3% DSS intervention and underwent two FMTs during the DSS intervention.

### Colitis-associated CRC model

To establish the colitis-associated CRC model, SPF C57BL/6 mice were intraperitoneally injected with AOM (10 mg/kg), followed by DSS administration. For AOM/DSS treatment, mice were injected with AOM on the first day and subsequently challenged with 1.5% DSS for 1 week, followed by normal drinking water for 1 week. After three cycles of DSS intervention, mice were given UDCA (50 mg/kg body weight) three times a week for 3 weeks. For AOM/DSS prevention, mice were treated first with DSS and then gavaged with UDCA after a 1-week interval. Mice were harvested after three cycles of DSS intervention. $Apc^{Min/+}$ mice were challenged with 1.5% DSS for 7 days after 3 weeks of UDCA treatment, and UDCA intervention was continued until the end of the experiment.

### High-throughput 16S rRNA gene amplicon sequencing and analysis

Fecal genomic DNA from DSS-induced colitis and FMT experiments was extracted using the DNeasy Blood & Tissue Kit (QIAGEN, Germantown, MD). In brief, barcoded amplicons from the V3–V4 region were generated using 2-step PCR. In the first step, 10 ng genomic DNA was used as template for the first PCR with a total volume of 20 μL, using the 338F and 806R primers appended with Illumina adaptor sequences.[53] Subsequently, PCR products were purified, checked on a fragment analyzer, and quantified, followed by equimolar multiplexing, and sequencing on an Illumina Miseq PE300 platform with the paired-end (2×x) 300-bp protocol. Quantitative Insights into Microbial Ecology 2 (QIIME2) software was used for microbial analyses.[54] Reads were imported, quality filtered, and dereplicated with the q2-data2 plugin. Subsequently, the dada2 plugin was used with paired-end reads with truncation of the primer sequences and trimming of the reads. The sequences were classified using Greengenes (v.13.8) as a reference 16S rRNA gene database.[55,56] PCoA, LefSe, and Significant Species were performed using R (v.4.1.1). A similar microbiotic analysis procedure was applied to the fecal microbiome from a clinical dataset (SRP181937).

### Host RNA sequencing and analysis

Colonic samples were obtained from mice with treatment of UDCA or *A. muciniphila*. Total RNA was extracted from mesenteric tissue using Trizol reagent (Life Technologies, Carlsbad, CA, USA) and precipitated with isopropanol. The RNA sequencing (RNA-seq) libraries (non-strand specific, paired end) were prepared using the TruSeq RNA Sample Prep kit (Illumina, San Diego, CA), and the libraries were successfully constructed from mesenteric samples. To construct the RNA-seq libraries, at least 100 ng of the total RNA was transcribed into cDNA, and the quantities of the cDNA libraries were assessed by Nanodrop instrument (Thermo Fisher Scientific). Then we used a Covaris S220 system (Covaris, Woburn, MA) to generate sheared cDNA and quantified the cDNA by Nanodrop again to calculate the appropriate amount of cDNA for library construction. Sample-specific barcodes were added to each cDNA library and then pooled and sequenced on a HiSeq platform (Illumine, San Diego, CA) with a 2 × 100-bp HiSeq run. Differential expression analysis of two groups (two biological replicates per condition) was performed using the limma R package. Genes with adjusted $p < 0.05$ were assigned as differentially expressed.

### Cell culture

The murine macrophage cell line RAW264.7 and intestinal epithelial cell line IEC-6 were purchased from the American Type Culture Collection. Cells were cultured at 37°C in Dulbecco's modified Eagle's medium (Gibco, Thermo Fisher Scientific, St. Peters, MO) supplemented with 10% fetal bovine serum (Gibco, Thermo Fisher Scientific) in a 5% $CO_2$ atmosphere. For the mouse fecal microbiota stimulation experiments, the ratio of 1 mL saline per 50 mg feces was used for preparing homogeneous fecal suspensions, which were then centrifuged for 1 min at 500 rpm. Bacterially enriched supernatants were centrifugated at 13,000 × *g* for 5 min, and the supernatant was discarded. The fecal microbiota was collected after suspending the microbiota pellet in 1 mL PBS and inactivation at 65°C for 30 min. The cultured cells were stimulated by fecal microbiota at a MOI (multiplicity of infection) of 200 for 24 h, and RNA was extracted for quantitative real-time PCR analysis. For co-culture of stimulated RAW264.7 and IEC-6 cells, co-culture was performed with 6-well plates with 0.4-μm pore size chamber inserts (Corning).

In brief, 2 × 10^6 microbiota-stimulated RAW264.7 cells were seeded in the upper chamber well, and 1 × $10^6$ IEC-6 cells were added into the lower chamber. After 24 h, IEC-6 cells were collected, and RNA was extracted for quantitative real-time PCR analysis.

#### Migration and invasion assays

Cell migration and invasion were examined using cell migration assays and a wound healing assay. Cell migration assays were performed with 24-well plates with 8-μm pore size chamber inserts (Corning). In general, 5 × $10^4$ IEC-6 cells resuspend in 200 μL serum-free DMEM were seeded in the upper chamber well, and 1 × 10^5 microbiota-stimulated RAW264.7 cells resuspend with 800 μL of DMEM with 10% FBS were added into the lower chamber. After 24 h, cells migrating through the membrane were fixed with 4% paraformaldehyde for 30 min and then stained with 0.1% crystal violet for 30 min. The cells were viewed under an inverted microscope (DMI4000B, Leica, Wetzlar, Germany) and we detected the absorbance at 570 nm after dissolving the crystal violet of the emigrated cells in a 33% acetic acid solution. The wound healing assay was performed with 12-well plates with 0.4-μm pore size chamber inserts (Corning). Generally, 1 × $10^5$ IEC-6 cells were distributed into each well of a 4-well scratcher in the lower chamber, and the scratcher was taken off after overnight apposition. 2 × 10^5 RAW264.7 cells stimulated with a bacterial suspension for 24 h were placed in the upper chamber for a total of 24 h. At 12 h and 24 h, the cells were viewed under an inverted microscope (DMI4000B, Leica, Wetzlar, Germany) and quantified using ImageJ.

#### RNA and DNA extraction

Colonic tissue samples were harvested, and RNA was extracted using a total RNA kit (RC112-01; Vazyme, China). cDNA was reverse transcribed using Hiscript@ III RT Super Mix with gDNA Wiper (R323-01; Vazyme, China). Fecal DNA was extracted using an AmPure Microbial DNA Kit (D7111; Megan, China).

#### Quantitative real-time PCR analysis

Quantitative real-time PCR was performed on an Applied Biosystems 7500 real-time PCR system using 2× SYBR Green Fast qPCR Mix (RK02001; Biomarker, China). The primer sequences used in this study are listed in Table S1.

#### Immunohistochemistry

Tissues were fixed in 4% formalin and embedded in paraffin. The sections were deparaffinized with dimethylbenzene and rehydrated using a graded alcohol series, followed by antigen retrieval and endogenous peroxidase quenching by $H_2O_2$. Sections were then blocked with normal goat serum for 30 min and incubated with Ki67 antibody (1:2,000, ab16667, Abcam, Cambridge, MA) overnight at 4°C. After washing three times with PBS, sections were incubated with the appropriate secondary antibodies (horseradish peroxidase [HRP] goat anti-rabbit immunoglobulin G [IgG], PV-6001, ZSGB-BIO, China) at a 1:500 dilution for 30 min at 37°C. Finally, sections were visualized by incubation in 3,3′-diaminobenzidine with 0.05% $H_2O_2$ for 1 min to induce a colorimetric reaction.

#### Western blotting

Radio-immunoprecipitation assay buffer consisting of 150 mM NaCl, 1% Triton X-100, 0.5% sodium deoxycholate, 0.1% sodium dodecyl sulfate, 50 mM Tris (pH 8), and protease inhibitor cocktail (Promega, Fitchburg, WI) was used to lyse cells. Sodium dodecyl sulfate-polyacrylamide gel electrophoresis was performed to separate the proteins, which were then transferred to polyvinylidene fluoride membranes using the Trans-Blot System (Bio-Rad, CA). The membranes were incubated with specific primary antibodies against ZO-1 (Abcam, ab96587), claudin 3 (Abcam, ab199635), occludin (Abcam, ab167161), and Glyceraldehyde 3-phosphate dehydrogenase (GAPDH) (Abcam, ab181602) at 4°C overnight after the membranes were blocked with 5% (w/v) skim milk (BD Biosciences, San Jose, CA) in Tris-buffered saline with 0.1% (v/v) Tween 20 (TBST) at room temperature for 1 h. The membranes were then washed with TBST three times and incubated with a specific secondary antibody (HRP goat anti-rabbit IgG, BA1054, Boster, China) at room temperature for 1 h. Enhanced chemiluminescence (ECL) Blotting Detection Reagents (Amersham Biosciences, Little Chalfont, Buckinghamshire, UK) were used to visualize the specific bands. GAPDH served as a control for the western blot analysis.

#### Quantification and statistical analysis

Unless otherwise stated, all statistical analyses were performed using Prism 8 (GraphPad, San Diego, CA). Two-tailed Student's t test (parametric) or Mann-Whitney U test (non-parametric) were applied. For comparison of more than three groups, statistical analysis was performed using one-way ANOVA (parametric) or Kruskal-Wallis test (non-parametric). All p values were two sided, and adjusted $p < 0.05$ was considered statistically significant. Details of the statistical tests are indicated in the respective figure legends. Statistical significance values are denoted as follows: *$p < 0.05$, **$p < 0.01$, ***$p < 0.001$, and ****$p < 0.0001$.

## ETHICS STATEMENT

Animals were handled in accordance with protocols approved by the IACUC at Sun Yat-Sen University.

## AVAILABILITY OF DATA AND MATERIAL

Data are available on reasonable request. All data relevant to the study are included in the article or uploaded as supplemental information.

## SUPPLEMENTAL INFORMATION

Supplemental information can be found online at https://doi.org/10.1016/j.ymthe.2022.10.014.

## ACKNOWLEDGMENTS

This study was supported by the National Key R&D Program of China (2017YFC1308800 to P.L.); the National Natural Science Foundation of China (81970452 to P.L., 81902938 to Z.H., and 82100588 to J.G.); the Science and Technology Program of Shenzhen, China (JCYJ20190807161807867 to P.L.); the Natural Science Foundation of Guangdong Province, China (2020A1515011248 to Z.H.); Fundamental Research Funds for the Central Universities (19ykzd02 to

Z.H.); and the Guang Dong Cheung Kong Philanthropy Foundation. The study sponsors did not play any role in the study design, sample collection, data analysis, data interpretation, or *in vitro* and *in vivo* experiments.

## AUTHOR CONTRIBUTIONS

Q.H., investigation, methodology, visualization, project administration, and writing – original draft; J.J., investigation, methodology, visualization, project administration, and writing – original draft; J.K., resources, methodology, formal analysis, data curation, and writing – review & editing; Q.Z., investigation, methodology, data curation, and formal analysis; W.Z., investigation, methodology, data curation, and formal analysis; Z.L., methodology and formal analysis; J.G., investigation, methodology, formal analysis, and funding acquisition; Y.C., resources and formal analysis; Z.H., conceptualization, supervision, funding acquisition, validation, writing – review & editing; P.L., conceptualization, supervision, funding acquisition, validation, and writing – review & editing.

## DECLARATION OF INTERESTS

The authors declare no competing interests.

## REFERENCES


1. Siegel, R.L., Miller, K.D., Goding Sauer, A., Fedewa, S.A., Butterly, L.F., Anderson, J.C., Cercek, A., Smith, R.A., and Jemal, A. (2020). Colorectal cancer statistics, 2020. CA. Cancer J. Clin. *70*, 145–164.
2. Keum, N., and Giovannucci, E. (2019). Global burden of colorectal cancer: emerging trends, risk factors and prevention strategies. Nat. Rev. Gastroenterol. Hepatol. *16*, 713–732.
3. Jess, T., Rungoe, C., and Peyrin-Biroulet, L. (2012). Risk of colorectal cancer in patients with ulcerative colitis: a meta-analysis of population-based cohort studies. Clin. Gastroenterol. Hepatol. *10*, 639–645.
4. Biondi, A., Zoccali, M., Costa, S., Troci, A., Contessini-Avesani, E., and Fichera, A. (2012). Surgical treatment of ulcerative colitis in the biologic therapy era. World J. Gastroenterol. *18*, 1861–1870.
5. Ungaro, R., Mehandru, S., Allen, P.B., Peyrin-Biroulet, L., and Colombel, J.F. (2017). Ulcerative colitis. Lancet *389*, 1756–1770.
6. Rooks, M.G., and Garrett, W.S. (2016). Gut microbiota, metabolites and host immunity. Nat. Rev. Immunol. *16*, 341–352.
7. Marchesi, J.R., Adams, D.H., Fava, F., Hermes, G.D.A., Hirschfield, G.M., Hold, G., Quraishi, M.N., Kinross, J., Smidt, H., Tuohy, K.M., et al. (2016). The gut microbiota and host health: a new clinical frontier. Gut *65*, 330–339.
8. Yang, Y., Li, L., Xu, C., Wang, Y., Wang, Z., Chen, M., Jiang, Z., Pan, J., Yang, C., Li, X., et al. (2020). Cross-talk between the gut microbiota and monocyte-like macrophages mediates an inflammatory response to promote colitis-associated tumourigenesis. Gut *70*, 1495–1506.
9. Quinn, R.A., Melnik, A.V., Vrbanac, A., Fu, T., Patras, K.A., Christy, M.P., Bodai, Z., Belda-Ferre, P., Tripathi, A., Chung, L.K., et al. (2020). Global chemical effects of the microbiome include new bile-acid conjugations. Nature *579*, 123–129.
10. Song, X., Sun, X., Oh, S.F., Wu, M., Zhang, Y., Zheng, W., Geva-Zatorsky, N., Jupp, R., Mathis, D., Benoist, C., and Kasper, D.L. (2020). Microbial bile acid metabolites modulate gut RORγ(+) regulatory T cell homeostasis. Nature *577*, 410–415.
11. Hang, S., Paik, D., Yao, L., Kim, E., Trinath, J., Lu, J., Ha, S., Nelson, B.N., Kelly, S.P., Wu, L., et al. (2019). Bile acid metabolites control T(H)17 and T(reg) cell differentiation. Nature *576*, 143–148.
12. Carey, E.J., Ali, A.H., and Lindor, K.D. (2015). Primary biliary cirrhosis. Lancet *386*, 1565–1575.
13. Pearson, T., Caporaso, J.G., Yellowhair, M., Bokulich, N.A., Padi, M., Roe, D.J., Wertheim, B.C., Linhart, M., Martinez, J.A., Bilagody, C., et al. (2019). Effects of ursodeoxycholic acid on the gut microbiome and colorectal adenoma development. Cancer Med. *8*, 617–628.
14. Low, E.N.D., Mokhtar, N.M., Wong, Z., and Raja Ali, R.A. (2019). Colonic mucosal transcriptomic changes in patients with long-duration ulcerative colitis revealed colitis-associated cancer pathways. J. Crohns Colitis *13*, 755–763.
15. Desai, A.A., Lei, Z., Bahroos, N., Maienschein-Cline, M., Saraf, S.L., Zhang, X., Shah, B.N., Nouraie, S.M., Abbasi, T., Patel, A.R., et al. (2017). Association of circulating transcriptomic profiles with mortality in sickle cell disease. Blood *129*, 3009–3016.
16. Lavelle, A., and Sokol, H. (2020). Gut microbiota-derived metabolites as key actors in inflammatory bowel disease. Nat. Rev. Gastroenterol. Hepatol. *17*, 223–237.
17. Liu, Q., Jiang, Z., Teng, Q., and Jiang, M. (2022). Pseudomembranous colitis caused by Haemophilus parainfluenzae. Inflamm. Bowel Dis. *28*, e55–e56.
18. Figliuolo, V.R., Dos Santos, L.M., Abalo, A., Nanini, H., Santos, A., Brittes, N.M., Bernardazzi, C., de Souza, H.S.P., Vieira, L.Q., Coutinho-Silva, R., and Coutinho, C.M.L.M. (2017). Sulfate-reducing bacteria stimulate gut immune responses and contribute to inflammation in experimental colitis. Life Sci. *189*, 29–38.
19. Dziarski, R., Park, S.Y., Kashyap, D.R., Dowd, S.E., and Gupta, D. (2016). Pglyrp-regulated gut microflora Prevotella falsenii, parabacteroides distasonis and Bacteroides eggerthii enhance and Alistipes finegoldii attenuates colitis in mice. PLoS One *11*, e0146162.
20. Zhao, Z.X., Yuan, X., Cui, Y.Y., Liu, J., Shen, J., Jin, B.Y., Feng, B.C., Zhai, Y.J., Zheng, M.Q., Kou, G.J., et al. (2021). Melatonin mitigates oxazolone-induced colitis in microbiota-dependent manner. Front. Immunol. *12*, 783806.
21. Ding, L., Yang, L., Wang, Z., and Huang, W. (2015). Bile acid nuclear receptor FXR and digestive system diseases. Acta Pharm. Sin. B *5*, 135–144.
22. Cani, P.D., and de Vos, W.M. (2017). Next-generation beneficial microbes: the case of Akkermansia muciniphila. Front. Microbiol. *8*, 1765.
23. Francis, M., Guo, G., Kong, B., Abramova, E.V., Cervelli, J.A., Gow, A.J., Laskin, J.D., and Laskin, D.L. (2020). Regulation of lung macrophage activation and oxidative stress following ozone exposure by farnesoid X receptor. Toxicol. Sci. *177*, 441–453.
24. He, Z., Gharaibeh, R.Z., Newsome, R.C., Pope, J.L., Dougherty, M.W., Tomkovich, S., Pons, B., Mirey, G., Vignard, J., Hendrixson, D.R., and Jobin, C. (2019). Campylobacter jejuni promotes colorectal tumorigenesis through the action of cytolethal distending toxin. Gut *68*, 289–300.
25. Tung, B.Y., Emond, M.J., Haggitt, R.C., Bronner, M.P., Kimmey, M.B., Kowdley, K.V., and Brentnall, T.A. (2001). Ursodiol use is associated with lower prevalence of colonic neoplasia in patients with ulcerative colitis and primary sclerosing cholangitis. Ann. Intern. Med. *134*, 89–95.
26. Serfaty, L., De Leusse, A., Rosmorduc, O., Desaint, B., Flejou, J.F., Chazouilleres, O., Poupon, R.E., and Poupon, R. (2003). Ursodeoxycholic acid therapy and the risk of colorectal adenoma in patients with primary biliary cirrhosis: an observational study. Hepatology *38*, 203–209.
27. Alberts, D.S., Martínez, M.E., Hess, L.M., Einspahr, J.G., Green, S.B., Bhattacharyya, A.K., Guillen, J., Krutzsch, M., Batta, A.K., Salen, G., et al. (2005). Phase III trial of ursodeoxycholic acid to prevent colorectal adenoma recurrence. J. Natl. Cancer Inst. *97*, 846–853.
28. Ward, J.B.J., Lajczak, N.K., Kelly, O.B., O'Dwyer, A.M., Giddam, A.K., Ní Gabhann, J., Franco, P., Tambuwala, M.M., Jefferies, C.A., Keely, S., et al. (2017). Ursodeoxycholic acid and lithocholic acid exert anti-inflammatory actions in the colon. Am. J. Physiol. Gastrointest. Liver Physiol. *312*, G550–G558.
29. Gao, R.Y., Shearn, C.T., Orlicky, D.J., Battista, K.D., Alexeev, E.E., Cartwright, I.M., Lanis, J.M., Kostelecky, R.E., Ju, C., Colgan, S.P., and Fennimore, B.P. (2021). Bile acids modulate colonic MAdCAM-1 expression in a murine model of combined cholestasis and colitis. Mucosal Immunol. *14*, 479–490.
30. Zhang, H., Xu, H., Zhang, C., Tang, Q., and Bi, F. (2021). Ursodeoxycholic acid suppresses the malignant progression of colorectal cancer through TGR5-YAP axis. Cell Death Discov. *7*, 207.
31. Wali, R.K., Stoiber, D., Nguyen, L., Hart, J., Sitrin, M.D., Brasitus, T., and Bissonnette, M. (2002). Ursodeoxycholic acid inhibits the initiation and postinitiation phases of

azoxymethane-induced colonic tumor development. Cancer Epidemiol. Biomarkers Prev. *11*, 1316–1321.

32. Kim, E.K., Cho, J.H., Kim, E., and Kim, Y.J. (2017). Ursodeoxycholic acid inhibits the proliferation of colon cancer cells by regulating oxidative stress and cancer stem-like cell growth. PLoS One *12*, e0181183.
33. Thompson, P.A., Wertheim, B.C., Roe, D.J., Ashbeck, E.L., Jacobs, E.T., Lance, P., Martínez, M.E., and Alberts, D.S. (2009). Gender modifies the effect of ursodeoxycholic acid in a randomized controlled trial in colorectal adenoma patients. Cancer Prev. Res. *2*, 1023–1030.
34. Islam, K.B.M.S., Fukiya, S., Hagio, M., Fujii, N., Ishizuka, S., Ooka, T., Ogura, Y., Hayashi, T., and Yokota, A. (2011). Bile acid is a host factor that regulates the composition of the cecal microbiota in rats. Gastroenterology *141*, 1773–1781.
35. Kurdi, P., Kawanishi, K., Mizutani, K., and Yokota, A. (2006). Mechanism of growth inhibition by free bile acids in lactobacilli and bifidobacteria. J. Bacteriol. *188*, 1979–1986.
36. Buffie, C.G., Bucci, V., Stein, R.R., McKenney, P.T., Ling, L., Gobourne, A., No, D., Liu, H., Kinnebrew, M., Viale, A., et al. (2015). Precision microbiome reconstitution restores bile acid mediated resistance to Clostridium difficile. Nature *517*, 205–208.
37. Van den Bossche, L., Hindryckx, P., Devisscher, L., Devriese, S., Van Welden, S., Holvoet, T., Vilchez-Vargas, R., Vital, M., Pieper, D.H., Vanden Bussche, J., et al. (2017). Ursodeoxycholic acid and its taurine- or glycine-conjugated species reduce colitogenic dysbiosis and equally suppress experimental colitis in mice. Appl. Environ. Microbiol. *83*, 027666-16.
38. Wang, L., Tang, L., Feng, Y., Zhao, S., Han, M., Zhang, C., Yuan, G., Zhu, J., Cao, S., Wu, Q., et al. (2020). A purified membrane protein from Akkermansia muciniphila or the pasteurised bacterium blunts colitis associated tumourigenesis by modulation of CD8(+) T cells in mice. Gut *69*, 1988–1997.
39. Juárez-Fernández, M., Porras, D., Petrov, P., Román-Sagüillo, S., García-Mediavilla, M.V., Soluyanova, P., Martínez-Flórez, S., González-Gallego, J., Nistal, E., Jover, R., and Sánchez-Campos, S. (2021). The synbiotic combination of Akkermansia muciniphila and quercetin ameliorates early obesity and NAFLD through gut microbiota reshaping and bile acid metabolism modulation. Antioxidants (Basel) *10*, 2001.
40. Jang, Y.J., Kim, W.K., Han, D.H., Lee, K., and Ko, G. (2019). Lactobacillus fermentum species ameliorate dextran sulfate sodium-induced colitis by regulating the immune response and altering gut microbiota. Gut Microbes *10*, 696–711.
41. Rodrigues, R.R., Gurung, M., Li, Z., García-Jaramillo, M., Greer, R., Gaulke, C., Bauchinger, F., You, H., Pederson, J.W., Vasquez-Perez, S., et al. (2021). Transkingdom interactions between Lactobacilli and hepatic mitochondria attenuate western diet-induced diabetes. Nat. Commun. *12*, 101.
42. Everard, A., Belzer, C., Geurts, L., Ouwerkerk, J.P., Druart, C., Bindels, L.B., Guiot, Y., Derrien, M., Muccioli, G.G., Delzenne, N.M., et al. (2013). Cross-talk between Akkermansia muciniphila and intestinal epithelium controls diet-induced obesity. Proc. Natl. Acad. Sci. USA *110*, 9066–9071.
43. Goossens, J.F., and Bailly, C. (2019). Ursodeoxycholic acid and cancer: from chemoprevention to chemotherapy. Pharmacol. Ther. *203*, 107396.
44. Barcelo, A., Claustre, J., Moro, F., Chayvialle, J.A., Cuber, J.C., and Plaisancié, P. (2000). Mucin secretion is modulated by luminal factors in the isolated vascularly perfused rat colon. Gut *46*, 218–224.
45. Smirnova, M.G., Guo, L., Birchall, J.P., and Pearson, J.P. (2003). LPS up-regulates mucin and cytokine mRNA expression and stimulates mucin and cytokine secretion in goblet cells. Cell. Immunol. *221*, 42–49.
46. Willemsen, L.E.M., Koetsier, M.A., van Deventer, S.J.H., and van Tol, E.A.F. (2003). Short chain fatty acids stimulate epithelial mucin 2 expression through differential effects on prostaglandin E(1) and E(2) production by intestinal myofibroblasts. Gut *52*, 1442–1447.
47. Hardbower, D.M., Coburn, L.A., Asim, M., Singh, K., Sierra, J.C., Barry, D.P., Gobert, A.P., Piazuelo, M.B., Washington, M.K., and Wilson, K.T. (2017). EGFR-mediated macrophage activation promotes colitis-associated tumorigenesis. Oncogene *36*, 3807–3819.
48. Huo, X., Li, D., Wu, F., Li, S., Qiao, Y., Wang, C., Wang, Y., Zhou, C., Sun, L., Luan, Z., et al. (2022). Cultivated human intestinal fungus Candida metapsilosis M2006B attenuates colitis by secreting acyclic sesquiterpenoids as FXR agonists. Gut *71*, 2205–2217.
49. Pathak, P., Xie, C., Nichols, R.G., Ferrell, J.M., Boehme, S., Krausz, K.W., Patterson, A.D., Gonzalez, F.J., and Chiang, J.Y.L. (2018). Intestine farnesoid X receptor agonist and the gut microbiota activate G-protein bile acid receptor-1 signaling to improve metabolism. Hepatology *68*, 1574–1588.
50. Cooper, H.S., Murthy, S.N., Shah, R.S., and Sedergran, D.J. (1993). Clinicopathologic study of dextran sulfate sodium experimental murine colitis. Lab. Invest. *69*, 238–249.
51. Klopfleisch, R. (2013). Multiparametric and semiquantitative scoring systems for the evaluation of mouse model histopathology–a systematic review. BMC Vet. Res. *9*, 123.
52. Lai, H.C., Lin, T.L., Chen, T.W., Kuo, Y.L., Chang, C.J., Wu, T.R., Shu, C.C., Tsai, Y.H., Swift, S., and Lu, C.C. (2022). Gut microbiota modulates COPD pathogenesis: role of anti-inflammatory Parabacteroides goldsteinii lipopolysaccharide. Gut *71*, 309–321.
53. Kozich, J.J., Westcott, S.L., Baxter, N.T., Highlander, S.K., and Schloss, P.D. (2013). Development of a dual-index sequencing strategy and curation pipeline for analyzing amplicon sequence data on the MiSeq Illumina sequencing platform. Appl. Environ. Microbiol. *79*, 5112–5120.
54. Kuczynski, J., Stombaugh, J., Walters, W.A., González, A., Caporaso, J.G., and Knight, R. (2012). Using QIIME to analyze 16S rRNA gene sequences from microbial communities. Curr. Protoc. Microbiol. *Chapter 1*, Unit.1E.5.
55. Edgar, R.C. (2010). Search and clustering orders of magnitude faster than BLAST. Bioinformatics *26*, 2460–2461.
56. DeSantis, T.Z., Hugenholtz, P., Larsen, N., Rojas, M., Brodie, E.L., Keller, K., Huber, T., Dalevi, D., Hu, P., and Andersen, G.L. (2006). Greengenes, a chimera-checked 16S rRNA gene database and workbench compatible with ARB. Appl. Environ. Microbiol. *72*, 5069–5072.